ISSN 1070-3284, Russian Journal of Coordination Chemistry, 2013, Vol. 39, No. 8, pp. 560–564. © Pleiades Publishing, Ltd., 2013.

Synthesis, Crystal Structure, and in vitro Antitumor Activity of a Novel Tetranuclear Di-*n*-Butyltin(IV)[1]

H. B. He[a], X. L. Ge[a], and B. F. Ruan[b, *]

[a] *School of Chemical Engineering, Hefei University of Technology, Hefei, 230009 P.R. China*

[b] *School of Medical Engineering, Hefei University of Technology, Hefei, 230009 P.R. China*

**e-mail: bf_ruan@163.com*

Received December 26, 2011

Abstract—A di-*n*-butyltin(IV) complex with (*E*)-3-(4-(9*H*-carbazole-9-yl)phenyl) acrylic acid (HL) of the formula $\{[n\text{-}Bu_2SnOL]_2O\}_2$ was synthesized and characterized by X-ray crystallography. This complex is a tetranuclear one with ladder framework. Furthermore, this complex was tested in vitro for its cytotoxic activity, using human hepatocellular carcinoma cell line (BEL-7402) and human hepatocellular liver carcinoma cell line (HepG2); 5-Fluorouracil was used as a positive control substance. This complex showed cytotoxicity greater than that of 5-Fluorouracil.

DOI: 10.1134/S1070328413070026

INTRODUCTION

Since the discovery of the antitumor activity of cisplatin during the 1960s, the application of metal complexes in the treatment of numerous human diseases has been a vigorously expanding area in biomedical and inorganic chemistry research [1]. The DNA nitrogen base binding cispaltin, oxalylplatin, nedaplatin, and carboplatin, all of which are metallocomplexes of platinum(II), have been proved to be the most effective and widely used coordination compounds as anticancer drugs [2]. In spite of its high activity, the application of cisplatin and its analogues has significant disadvantages that include: (1) poor water solubility, (2) severe side effects that are typical of heavy metals toxicity, and (3) the development of drug tolerance by the tumor [3]. The last two are the major driving force behind current research in the field of novel anticancer agent development.

Organotin(IV) carboxylates comprises the class of tin complexes which has attracted particular attention due to their potential cytotoxicity and biocide activity as well as their industrial and agricultural applications [4–7]. Our recent efforts have focused on the aspects of synthesis and biological activity of new organotin(IV) complexes with different RCOOH (R = carbazole) as ligands. Herein we report the synthesis and characterization of a new organotin(IV) complex $\{[n\text{-}Bu_2SnOL]_2O\}_2$ (**I**) derived from a carbazole carboxylic acid. We also report its in vitro cytotoxicity in hepatocellular carcinoma (BEL-7402) and human hepatocellular liver carcinoma cell line (HepG2), and some preliminary structure-activity relationships are discussed.

[1] The article is published in the original.

EXPERIMENTAL

The organotin(IV) precursor $n\text{-}Bu_2SnO$ was purchased from Aldrich and were used without further purification. All the solvents were dried according to reported procedures. The ligand was synthesized by the methods as reported [8, 9]. Melting points were determined on an Electrothermal Mettler-Toledo (FP62) instrument. ^1H and ^{13}C NMR were recorded at Bruker AV 400 spectrometer at 25°C with TMS and solvent signals allotted as internal standards. ^{119}Sn NMR spectra (proton-decoupled) were recorded on a Bruker AV 400 spectrometer operating at 150 MHz; resonances are referenced to tetramethyltin (external standard, ^{119}Sn). Elemental analyses were performed on a CHN–O-Rapid instrument and were within ±0.4% of the theoretical values. IR spectra were record on a Nicolet 470 FT-IR spectrophotometer using KBr pellets in the range from 4000 to 400 cm^{-1}.

Synthesis of complex I was carried out according to the following scheme:

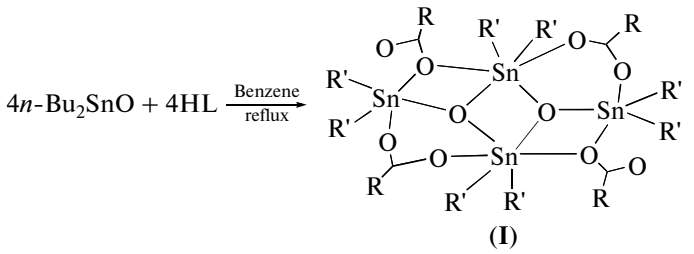

(I)

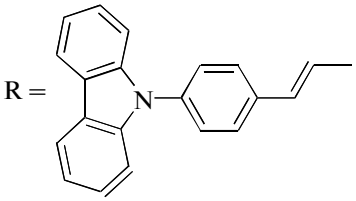

To a benzene solution (25 mL) of n-Bu_2SnO (0.249 g, 1 mmol), HL (0.313 g, 1 mmol) was added at room temperature. After addition, the reaction mixture refluxed for 24 h with stirring and then filtered; the solvent was removed under vacuum and the residue was dissolved in CH_2Cl_2 (10 mL) and filtered. Colorless crystals of complex I were obtained by evaporating slowly in dichloromethane–ethyl ether (3 : 1) solutions at room temperature. The yield was 80.0%, m.p. > 300°C.

For $C_{116}H_{128}N_4O_{10}Sn_4$			
anal. calcd., %:	C, 62.95;	H, 5.83;	N, 2.53.
Found, %:	C, 63.17;	H, 5.85;	N, 2.54.

^{1}H NMR (400 Hz; $CDCl_3$; δ, ppm): 1.01 (t., J = 7.2 Hz, 24H), 1.48–1.86 (m., 48H), 6.58 (d., J = 16 Hz, 4H), 7.33 (d., J = 16 Hz, 4H), 7.25–8.17 (ArH, 48H). ^{13}C NMR ($CDCl_3$; δ, ppm): 9.05, 22.18, 22.81, 23.13, 105.03, 105.84, 114.67, 115.62, 118.88, 121.08, 121.35, 124.67, 135.75.

^{119}Sn NMR ($CDCl_3$; δ, ppm): –147.3 and –216.2.

IR (KBr; ν, cm^{-1}): 1641 ν_s(C=O), 570 ν(Sn–O), 620 ν(O–Sn–O).

X-ray structure determination. Single crystal X-ray diffraction measurements were carried out on a Siemens Smart 1000 CCD diffractmeter equipped with a graphite crystal monochromator situated in the incident beam for data collection at room temperature. The determination of unit cell parameters and data collections were performed with MoK_α radiation (λ = 0.71073 Å). Unit cell dimensions were obtained with least-squares refinements, and all structures were solved by direct methods with SHELXL-97. All the non-hydrogen atoms were located in successive difference Fourier syntheses. The final refinement was performed by full-matrix least-squares methods with anisotropic thermal parameters for non-hydrogen atoms on F^2. The hydrogen atoms were added theoretically and riding on the concerned atoms. The crystal data and structure refinement for complex **I** were listed in Table 1.

Supplementary material for structure **I** has been deposited with the Cambridge Crystallographic Data Centre (no. 704782; deposit@ccdc.cam.ac.uk or http://www.ccdc.cam.ac.uk).

Table 1. Crystallographic data and structure refinement for complex **I**

Parameter	Value
M	2213.12
Crystal system	Triclinic
Space group	$P\bar{1}$
Crystal size, mm	0.38 × 0.35 × 0.14
a, Å	14.073(4)
b, Å	14.498(4)
c, Å	14.576(4)
α, deg	86.092(4)
β, deg	75.244(3)
γ, deg	71.952(4)
Volume, Å^3	2734.1(13)
Z	1
ρ_c, g cm^{-3}	1.363
μ, mm^{-1}	0.960
F(000)	1148
θ Range of data collected, deg	1.77–25.30
Reflections collected	14181
Reflections unique (R_{int})	9508 (0.0414)
Parameters	618
Goodness-of-fit on F^2	1.003
R_1, wR_2 ($I > 2\sigma(I)$)	0.064, 0.1756
R_1, wR_2 (all data)	0.145, 0.2336
Largest diff. peak and hole, e Å^{-3}	2.308/–0.717

Table 2. Selected bond lengths (Å) and angles (deg) for complex **I**

Bond	*d*, Å	Bond	*d*, Å
Sn(1)–O(1)	2.826(8)	Sn(1)–O(4*A*)	2.249(1)
Sn(1)–O(5)	2.175(8)	Sn(1)–O(5*A*)	2.041(6)
Sn(2)–O(3)	2.237(8)	Sn(2)–O(5)	2.012(8)
Sn(2)–O(1)	2.170(8)	Sn(1)–Sn(1*A*)	3.297(1)
Angle	ω, deg	Angle	ω, deg
O(1)C(22)O(2)	121.8(1)	C(22)O(1)Sn(2)	117.6(7)
O(1)Sn(2)O(5)	81.3(3)	O(1)Sn(1)O(5)	64.5(2)
Sn(2)O(5)Sn(1)	120.9(3)	Sn(1)O(5)Sn(1*A*)	102.9(3)
Sn(1)O(5*A*)Sn(2*A*)	136.2(4)	O(1)Sn(1)O(4*A*)	130.6(3)
O(3)C(1)O(4)	122.8(1)	O(5)Sn(2)O(3)	100.2(2)

Cytotoxicity assay against BEL-7402 and HepG2. The cytotoxicity of the prepared complex against human hepatocellular carcinoma cell line (BEL-7402) and human hepatocellular liver carcinoma cell line (HepG2) was evaluated as described elsewhere with some modifications [10]. Briefly, target tumor cells were grown to log phase in RPMI 1640 medium supplemented with 10% fetal bovine serum. After diluting to 2×10^4 cells mL^{-1} with the complete medium, 100 μL of the obtained cell suspension was added to each well of 96-well culture plates. The subsequent incubation was permitted at 37°C, 5% CO_2 atmosphere for 24 h before the cytotoxicity assessments. Tested samples at pre-set concentrations were added to 6 wells with 5-fluorouracil co-assayed as a positive reference. After 48 h exposure period, 40 μL of PBS containing 2.5 mg mL^{-1} of MTT (3-(4,5-dimethylthiazol-2-yl)-2,5-diphenyltetrazolium bromide) was added to each well.

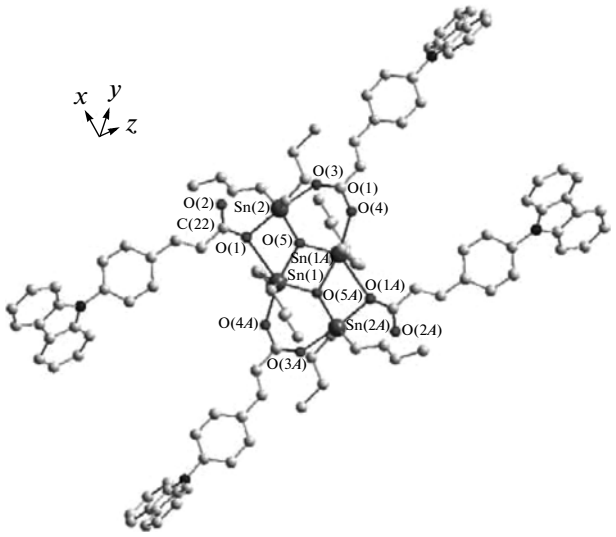

Fig. 1. Molecular structure of complex **I** (all hydrogen atoms are omitted for clarity).

Table 3. Cytotoxic activities of complex **I** against human tumor cells*

Complex	IC_{50} (μg/mL)	
	HepG2	BEL-7402
I	2.34 ± 0.35	1.21 ± 0.37
n-Bu_2SnO	20.26 ± 0.46	18.27 ± 0.68
HL	32.07 ± 0.15	29.20 ± 0.21
5-Fluorouracil**	19.17 ± 0.38	17.43 ± 0.25

Notes: * Antitumor activities are expressed as IC_{50} (50% inhibitory concentration) toward the cell lines HepG2 and BEL-7402. Data are average data of triplicate assay.
** Used as a positive control.

Four hours later, 100 μL extraction solutions (10% SDS–5% isobutyl alcohol–0.01 M HCl) was added. After an overnight incubation at 37°C, the optical density was measured at a wavelength of 570 nm on an ELISA microplate reader. In all experiments three replicate wells were used for each drug concentration. Each assay was carried out at least three times.

RESULTS AND DISCUSSION

The IR spectrum of complex **I** indicates the complete disappearance of the stretching vibration bands of O–H of their free ligands and show characteristic absorptions at 1571–1641 cm^{-1} assigned to ν(C=O). These features are consistent with the double deprotonated carboxylic form of the ligand. For this complex, no ν(OH) band was detected, in accord with deprotonation and coordination to the metal of both oxygens of the ligands. The bands in the region at 536–566 cm^{-1} were assigned to ν(Sn–O). The bands in the region at 620–634 cm^{-1} were assigned to ν(Sn–O–Sn).

The values of ^{119}Sn chemical shift for the organotin(IV) compounds may be used to give tentative indications of the environment around tin atoms. As for complex **I**, the solution ^{119}Sn spectra show two signals, indicating the presence of two different types of tin sites of five- and six-coordinated in both complexes. It also reveals that the tetrameric structures found in the solid state retained in solution [11].

The molecular structure of **I** is shown in Fig. 1, and selected bond lengths and angles are given in Table 2. The crystal structure shows a ladder framework. The centrosymmetric structure features a central Sn_2O_2 core to which are linked two *n*-Bu_2Sn entities with the result that the O(1) and O(1*A*) atoms are three coordinate. The ligand is involved in both anisobidentate chelating (Sn(1)–O(1) 2.826(8) and Sn(2*A*)–O(1) 2.170(8) Å as well as isobidentate bridging coordination modes (Sn(1)–O(4) 2.2488(103) and Sn(2)–O(3) 2.2365(76) Å), falling in the rational Sn–O bond lengths). This lead to a situation where the endo tins

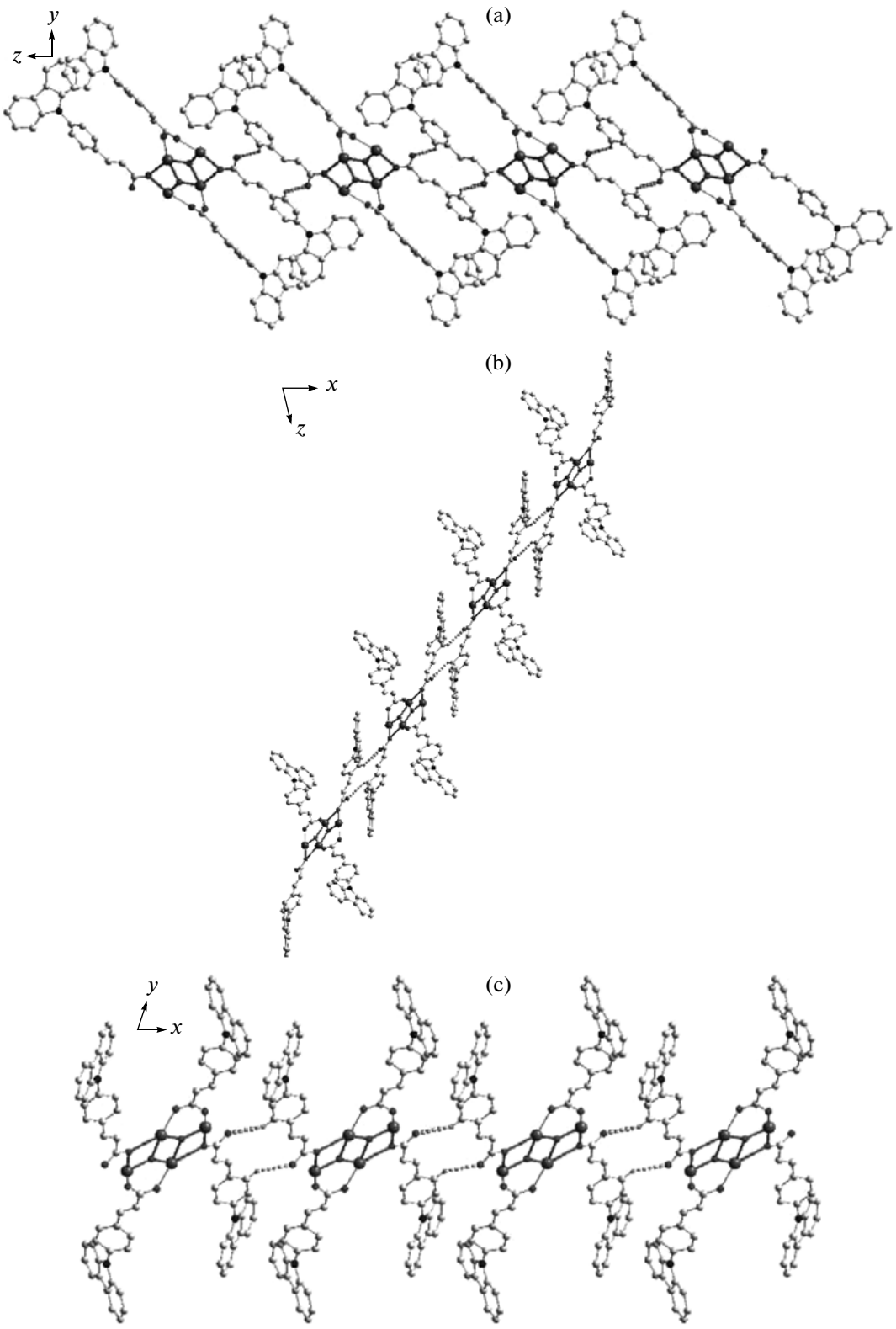

Fig. 2. View of the layers of complex **I**: along the *x* axis (a); the *y* axis (b); the *z* axis (c). Benzyl groups and all the H atoms are omitted for clarity.

are hexa-coordinate with a skew-trapezoidal geometry while the exo tins are pentacoordinated with distorted trigonal-bipyramidal geometry [12], which is a little different [13]. As shown in Fig. 2, intermolecular H bonds between adjacent molecules lead to a 1D chain structure. The bond length is 3.659 Å (C(27)···O(2)) and the bond angle is 136° (C(27)–H(27)···O(2)).

On the basis of the preliminary screening results (Table 3), it is evident that the di-*n*-butyltin(IV) derivatives is active against both the human hepatocellular carcinoma cell line (BEL-7402) and human hepatocellular liver carcinoma cell line (HepG2). For both the cell lines, the activity of complex **I** was actually greater than that for 5-Fluorouracil as well as the organotin(IV) precursor *n*-Bu_2SnO. It is reasonable that a weak Sn–O bond in complex **I** is the key factor because the further ligand replacement with biological ligands is possible [14]. The bond Sn(1)–O(1) with the length of 2.826 Å in complex **I** is much longer than other Sn–O bonds, indicating that the interaction between Sn(1)–O(1) is very weak. Hence, it is conceivable that ligand replacement from Sn–O–core cluster to Sn-DNA complex following the Sn–O cleavage for **I** is expected in this case, according to Huber and Saxena [15].

ACKNOWLEDGMENTS

This work was supported by the Fundamental Research Funds for the Central Universities (2012HGQC0034).

REFERENCES

1. Blower, P.J., *Annu. Rep. Prog. Chem., A*, 2001, vol. 97, p. 587.
2. Wong, E. and Giandomenico, C.M., *Chem. Rev.*, 1999, vol. 99, p. 2451.
3. Hadjikakou, S.K. and Hadjiliadis, N., *Coord. Chem. Rev.*, 2009, vol. 253, p. 235.
4. Molly, K.C., Purcell, T.G., Hahn, E., et al., *Organometallics*, 1986, vol. 5, p. 85.
5. Gielen, M., *Appl. Organomet. Chem.*, 2002, vol. 16, p. 481.
6. Gielen, M., Biesemans, M., and Willem, R., *Appl. Organomet. Chem.*, 2005, vol. 19, p. 440.
7. Gielen, M. and Braz, J., *Chem. Soc.*, 2003, vol. 14, p. 870.
8. Fousteris, M.A., Papakyriakou, A., Koutsourea, A., et al., *J. Med. Chem.*, 2008, vol. 1048, p. 51.
9. Wu, J.-Y., Pan, Y.-L., Zhang, X.-J., et al., *Inorg. Chim. Acta*, 2007, vol. 2083, p. 360.
10. Chen, X., Plasencia, C., Hou, Y., and Neamati, N., *J. Med. Chem.*, 2005, vol. 48, p. 1098.
11. Chandrasekhar, V., Nagendran, S., and Baskar, V., *Coord. Chem. Rev.*, 2002, vol. 235, p. 1.
12. Li, D.-M., Hu, R.-T., Zhou, W., et al., *Eur. J. Inorg. Chem.*, 2009, vol. 18, p. 2664.
13. Kovala-Demertzi, D., Dokorou, V., Primikiri, A., et al., *J. Inorg. Biochem.*, 2009, vol. 103, p. 738.
14. Willem, R., Dalil, H., Biesemans, M., et al., *Appl. Organomet. Chem.*, 1999, vol. 13, p. 605.
15. Saxena, A.K. and Huber, F., *Coord. Chem. Rev.*, 1989, vol. 95, p. 109.